J Biol Inorg Chem (2011) 16:97–108
DOI 10.1007/s00775-010-0706-2

ORIGINAL PAPER

Isoniazid and rifampicin inhibit allosterically heme binding to albumin and peroxynitrite isomerization by heme–albumin

Paolo Ascenzi · Alessandro Bolli · Alessandra di Masi · Grazia R. Tundo · Gabriella Fanali · Massimo Coletta · Mauro Fasano

Received: 28 April 2010 / Accepted: 27 August 2010 / Published online: 25 September 2010

Abstract Human serum heme–albumin (HSA-heme) displays globin-like properties. Here, the allosteric inhibition of ferric heme [heme-Fe(III)] binding to human serum albumin (HSA) and of ferric HSA–heme [HSA-heme-Fe(III)]-mediated peroxynitrite isomerization by isoniazid and rifampicin is reported. Moreover, the allosteric inhibition of isoniazid and rifampicin binding to HSA by heme-Fe(III) has been investigated. Data were obtained at pH 7.2 and 20.0 °C. The affinity of isoniazid and rifampicin for HSA [$K_0 = (3.9 \pm 0.4) \times 10^{-4}$ and $(1.3 \pm 0.1) \times 10^{-5}$ M, respectively] decreases by about 1 order of magnitude upon heme-Fe(III) binding to HSA [$K_h = (4.3 \pm 0.4) \times 10^{-3}$ and $(1.2 \pm 0.1) \times 10^{-4}$ M, respectively]. As expected, the heme-Fe(III) affinity for HSA [$H_0 = (1.9 \pm 0.2) \times 10^{-8}$ M] decreases by about 1 order of magnitude in the presence of saturating amounts of isoniazid and rifampicin [$H_d = (2.1 \pm 0.2) \times 10^{-7}$ M]. In the absence and presence of CO_2, the values of the second-order rate constant (l_{on}) for peroxynitrite isomerization by HSA-heme-Fe(III) are 4.1×10^5 and 4.3×10^5 M^{-1} s^{-1}, respectively. Moreover, isoniazid and rifampicin inhibit dose-dependently peroxynitrite isomerization by HSA-heme-Fe(III) in the absence and presence of CO_2. Accordingly, isoniazid and rifampicin impair in a dose-dependent fashion the HSA-heme-Fe(III)-based protection of free L-tyrosine against peroxynitrite-mediated nitration. This behavior has been ascribed to the pivotal role of Tyr150, a residue that either provides a polar environment in Sudlow's site I (i.e., the binding pocket of isoniazid and rifampicin) or protrudes into the heme-Fe(III) cleft, depending on ligand binding to Sudlow's site I or to the FA1 pocket, respectively. These results highlight the role of drugs in modulating heme-Fe(III) binding to HSA and HSA-heme-Fe(III) reactivity.

Electronic supplementary material The online version of this article (doi:10.1007/s00775-010-0706-2) contains supplementary material, which is available to authorized users.

P. Ascenzi (✉) · A. Bolli · A. di Masi
Department of Biology and Interdepartmental Laboratory for Electron Microscopy, University Roma Tre, Viale Guglielmo Marconi 446, 00146 Rome, Italy
e-mail: ascenzi@uniroma3.it

P. Ascenzi
National Institute for Infectious Diseases I.R.C.C.S. 'Lazzaro Spallanzani', Via Portuense 292, 00149 Rome, Italy

G. R. Tundo · M. Coletta
Department of Experimental Medicine and Biochemical Sciences, University of Roma 'Tor Vergata', Via Montpellier 1, 00133 Rome, Italy

G. R. Tundo · M. Coletta
Interuniversity Consortium for the Research on the Chemistry of Metals in Biological Systems, Via Celso Ulpiani 27, 70126 Bari, Italy

G. Fanali · M. Fasano
Department of Structural and Functional Biology, Center of Neuroscience, University of Insubria, Via Alberto da Giussano 12, 21052 Busto Arsizio (VA), Italy

Keywords Allostery · Ferric human serum heme–albumin · Human serum albumin · Isoniazid · Rifampicin

Abbreviations

FA	Fatty acid
Heme–Fe(III)	Ferric heme
HSA	Human serum albumin
HSA-heme	Human serum heme–albumin
HSA-heme-Fe(II)-NO	Ferrous nitrosylated human serum heme–albumin
HSA-heme-Fe(III)	Ferric human serum heme–albumin

Introduction

Human serum albumin (HSA) is the most abundant protein in plasma and provides a depot and carrier for many compounds. As a consequence, HSA affects the pharmacokinetics of many drugs, holds some ligands in a strained orientation that results in their metabolic modification, and renders potential toxins harmless, transporting them to disposal sites. Moreover, HSA accounts for most of the antioxidant capacity of human serum and displays enzymatic properties [1–9].

HSA is a single nonglycosylated all-α-chain protein, constituted by 585 amino acids, containing three homologous domains (labeled I, II, and III). Each domain is made up of two separate subdomains (named A and B) connected by random coils. Interdomain helical regions link subdomain IB to subdomain IIA and subdomain IIB to subdomain IIIA (Fig. 1) (see [2, 8–11]).

The structural organization of HSA provides several ligand binding sites (Fig. 1). HSA displays seven binding clefts hosting chemically diverse ligands including fatty acids (FAs), and are therefore labeled FA1–FA7 (Fig. 1). In particular, FA1 is located within the IB subdomain contacting the IB–IIA polypeptide linker and the long IB–IIA transdomain helix; FA2 is located at the interface between subdomains IA, IB, and IIA; FA3 and FA4 together contribute to Sudlow's site II (i.e., the ibuprofen primary site) in subdomain IIIA; FA5 is located within subdomains IIIA and IIIB; FA6 is a solvent-accessible linear slot located at the interface between subdomains IIA and IIB; and FA7 corresponds to Sudlow's site I (i.e., the warfarin binding site) in subdomain IIA. FA2 and FA6 clefts appear to be the secondary binding sites of ibuprofen. Moreover, HSA binds ligands (e.g., thyroxine) in the cleft between domains I and III and the bacterial HSA-binding modules to domain II [7, 9, 10, 12–19].

The FA1 binding site has evolved to selectively bind the ferric heme [heme-Fe(III)] with a high affinity

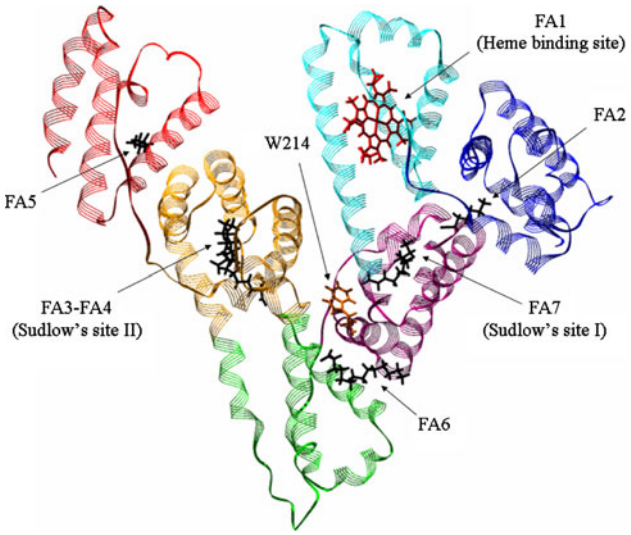

Fig. 1 Three-dimensional structure of human serum albumin (HSA). Subdomains are labeled as follows: *blue* IA, *cyan* IB, *purple* IIA, *green* IIB, *yellow* IIIA, and *red* IIIB. Ligand binding clefts are shown and labeled FA1–FA7; FA1 is occupied by the heme (*red sticks*), whereas FA2–FA7 are occupied by myristate ions (*black sticks*). The spectroscopically active Trp214 residue (W214) is rendered in *orange sticks* and labeled. FA7 corresponds to Sudlow's site I (i.e., the warfarin site). The FA3 and FA4 sites form Sudlow's site II (i.e., the ibuprofen site). Atomic coordinates were taken from Protein Data Bank code 1O9X [78]. For further details, see the text

($H_0 = 1.3 \times 10^{-8}$ M), so HSA participates physiologically to heme scavenging [20–23]. The tetrapyrrole ring is arranged in a D-shaped cavity limited by Tyr138 and Tyr161 residues that provide π–π stacking interaction with the porphyrin and supply a donor oxygen (from Tyr161) for the heme atom. The heme is secured to HSA by the long IA–IB connecting loop that fits into the cleft opening [9, 24–26]. In turn, heme endows HSA with reactivity and spectroscopic properties similar to those of hemoglobin and myoglobin [9, 12, 26–41]. Remarkably, both heme-Fe(III) binding to HSA and human serum heme–albumin (HSA-heme) reactivity are modulated allosterically [8, 9, 19, 24, 29, 32–34, 38, 39, 42, 43].

Here, the effect of isoniazid and rifampicin, two widely used antituberculosis drugs [44], on heme-Fe(III) binding to HSA and ferric HSA-heme [HSA-heme-Fe(III)]-mediated peroxynitrite[1] isomerization is reported. Isoniazid and rifampicin impair heme-Fe(III) binding to HSA and vice versa, according to linked functions [45]. Moreover, isoniazid and rifampicin inhibit dose-dependently peroxynitrite isomerization by HSA-heme-Fe(III), and the HSA-heme-Fe(III)-based protection of free L-tyrosine against

[1] The recommended IUPAC nomenclature for peroxynitrite is oxoperoxonitrate(1-) and for peroxynitrous acid is hydrogen oxoperoxonitrate. The term "peroxynitrite" is used in the text to refer generically to both $ONOO^-$ and its conjugate acid ONOOH (see [33, 53, 59, 77]).

peroxynitrite-mediated nitration. These results highlight the role of drugs in modulating both heme binding to HSA and HSA-heme reactivity.

Materials and methods

Materials

Hemin [iron(III) protoporphyrin IX] chloride was purchased from Sigma–Aldrich (St. Louis, MO, USA). The heme-Fe(III) stock solution (5.0×10^{-3} M) was prepared by dissolving heme-Fe(III) in 1.0×10^{-2} M NaOH [46]. The heme-Fe(III) concentration was determined spectrophotometrically at 535 nm after converting heme-Fe(III) to the heme-Fe(III) bisimidazolate derivative in sodium dodecyl sulfate micelles ($\varepsilon_{535\ nm} = 14.5 \times 10^3\ M^{-1}\ cm^{-1}$) [47].

HSA (purity 96% or better, essentially FA free) was obtained from Sigma–Aldrich. The HSA concentration was determined spectrophotometrically at 280 nm ($\varepsilon_{280\ nm} = 3.82 \times 10^4\ M^{-1}\ cm^{-1}$) [46]. The HSA stock solution (2.0×10^{-4} M) was prepared by diluting the hydrophobic ligand-free HSA solution with 2.0×10^{-2} M sodium phosphate buffer, at pH 7.2 and 20.0 °C. The HSA-heme-Fe(III) stock solution (2.0×10^{-4} M) was prepared by adding a 0.8 M defect of the heme-Fe(III) stock solution to the HSA solution (pH 7.2, 1.0×10^{-1} M sodium phosphate buffer) at 20.0 °C [33–36, 39–41, 46, 48]. The final HSA and HSA-heme-Fe(III) concentrations ranged between 1.0×10^{-8} and 5.0×10^{-6} M.

Isoniazid and rifampicin (Fig. S1) were purchased from Sigma–Aldrich. The isoniazid stock solution (2.0×10^{-1} M) was prepared by dissolving the drug in 95% water–5.0% methanol (v/v). The rifampicin stock solution (2.0×10^{-2} M) was prepared by dissolving the drug in methanol [49]. The final isoniazid and rifampicin concentrations ranged between 1.0×10^{-5} and 2.0×10^{-2} M and between 1.0×10^{-6} and 2.0×10^{-3} M, respectively.

Peroxynitrite was synthesized from KO_2 and NO and from HNO_2 and H_2O_2 and was stored in small aliquots at −80.0 °C [50, 51]. The peroxynitrite stock solution (2.0×10^{-3} M) was diluted immediately before use with degassed 5.0×10^{-2} M NaOH to reach the desired concentration [33, 48, 52–55]. Nitrate and nitrite contaminations were in the ranges 0–7% and 8–19% of the peroxynitrite concentration, respectively (see "Methods"). The concentration of peroxynitrite was determined spectrophotometrically prior to each experiment by measuring the absorbance at 302 nm ($\varepsilon_{302\ nm} = 1.705 \times 10^3\ M^{-1}\ cm^{-1}$) [50, 51, 55, 56].

Experiments in the presence of CO_2 were carried out by adding to the protein solutions the required amount of a 5.0×10^{-1} M $NaHCO_3$ solution. After the addition of bicarbonate, the protein solutions were allowed to equilibrate for at least 5 min [33, 48, 52–55]. For the experiments carried out in the absence of CO_2, all solutions were thoroughly degassed and kept under nitrogen or helium [33, 48, 52–55].

All the other chemicals were obtained from Sigma–Aldrich and Merck (Darmstadt, Germany). All products were of analytical or reagent grade and were used without further purification.

Methods

Isoniazid and rifampicin binding to HSA

Values of the dissociation equilibrium constant for isoniazid and rifampicin binding to HSA (i.e., K_0) were obtained spectrofluorimetrically at pH 7.2 (1.0×10^{-1} M phosphate buffer) and 20.0 °C. The intrinsic tryptophan fluorescence of HSA in the absence and presence of isoniazid and rifampicin was recorded between 290 and 700 nm; the excitation wavelength was 280 nm. The excitation and emission slit widths were 5 nm. Small aliquots of either isoniazid (2.0×10^{-1} M) or rifampicin (2.0×10^{-2} M) stock solutions were added to the HSA (5.0×10^{-6} M) solution, and the drug-dependent changes of the intrinsic fluorescence of HSA were recorded after incubation for 10 min after each addition. The intrinsic fluorescence of both drugs was recorded between 290 and 700 nm (the excitation wavelength was 280 nm) to evaluate the interference with the intrinsic tryptophan fluorescence of HSA [6, 21, 22, 57, 58]. No intrinsic fluorescence of isoniazid and rifampicin between 290 and 700 nm (the excitation wavelength was 280 nm) was observed. Test measurements performed after 2 h of HSA–drug incubation excluded slow kinetic effects.

Isoniazid and rifampicin binding to HSA was analyzed by plotting the molar fraction of the drug–HSA complex (i.e., Y) as a function of the free drug concentration. Data were analyzed according to Eq. 1 [6, 21, 22, 57, 58]:

$$Y = \Delta F/\Delta F_{max} = [drug]/(K_0 + [drug]) \quad (1)$$

where ΔF is the fluorescence change at a given drug concentration, and ΔF_{max} is the fluorescence change at the saturating drug concentration.

Isoniazid and rifampicin binding to HSA-heme-Fe(III)

Values of the dissociation equilibrium constant for isoniazid and rifampicin binding to HSA-heme-Fe(III) (i.e., K_h) were obtained spectrophotometrically at pH 7.2 (1.0×10^{-1} M phosphate buffer) and 20.0 °C. Heme-Fe(III)-based drug-dependent absorbance changes were recorded between 350 and 450 nm. Small aliquots of either isoniazid (2.0×10^{-1} M) or rifampicin (2.0×10^{-2} M) stock solutions were added to the HSA-heme-Fe(III) (5.0×10^{-6} M)

solution and the drug-dependent absorbance changes of HSA-heme-Fe(III) were recorded after incubation for 10 min after each addition [21, 22]. Test measurements performed after 2 h of HSA-heme-Fe(III)–drug incubation excluded slow kinetic effects.

Isoniazid and rifampicin binding to HSA-heme-Fe(III) was analyzed by plotting the molar fraction of the drug–HSA-heme-Fe(III) complex (i.e., Y) as a function of the free drug concentration. Data were analyzed according to Eq. 2 [21, 22]:

$$Y = \Delta A/\Delta A_{max} = [\text{drug}]/(K_h + [\text{drug}]) \quad (2)$$

where ΔA is the absorbance change at a given drug concentration, and ΔA_{max} is the absorbance change at the saturating drug concentration.

Heme-Fe(III) binding to HSA and HSA–drug complexes

Values of the dissociation equilibrium constant for heme-Fe(III) binding to HSA in the absence and presence of isoniazid and rifampicin (i.e., H_0 and H_d, respectively) were obtained spectrophotometrically at pH 7.2 (1.0×10^{-1} M phosphate buffer) and 20.0 °C. Heme-Fe(III)-dependent absorbance changes were recorded between 350 and 450 nm. Small aliquots of the HSA (2.0×10^{-4} M) stock solution were added to the heme-Fe(III) (5.0×10^{-7} M) solution in the absence and presence of isoniazid (3.0×10^{-5}–3.0×10^{-2} M) and rifampicin (3.0×10^{-6}–3.0×10^{-3} M). The heme-Fe(III)-dependent absorbance changes accompanying HSA-heme-Fe(III) formation were recorded after incubation for 10 min after each addition [21, 22]. Test measurements performed after 2 h of HSA-heme-Fe(III) and HSA-heme-Fe(III)–drug incubation excluded slow kinetic effects.

Heme-Fe(III) binding to HSA in the absence and presence of isoniazid and rifampicin was analyzed by plotting the molar fraction of HSA-heme-Fe(III) (i.e., Y) as a function of the HSA concentration. Data were analyzed according to Eq. 3 [21, 22]:

$$Y = \Delta A/\Delta A_{max} = [\text{HSA}]/(H + [\text{HSA}]) \quad (3)$$

where H corresponds to either H_0 or H_d.

The dependence of the dissociation equilibrium constant H for heme-Fe(III) binding to HSA as a function of the isoniazid or rifampicin concentration was analyzed according to Eq. 4 [21, 22, 45]:

$$\log H = \log H_d^{-1} + \log\{([\text{drug}] + K_h)/([\text{drug}] + K_0)\} \quad (4)$$

Peroxynitrite isomerization in the absence and presence of HSA-heme-Fe(III), CO_2, isoniazid, and rifampicin

The kinetics of peroxynitrite isomerization in the absence and presence of HSA-heme-Fe(III), CO_2, isoniazid, and rifampicin was recorded with SMF-20 and SMF-400 rapid-mixing stopped-flow apparatus (Bio-Logic, Claix, France). The light path of the observation cuvette was 10 mm, and the dead time was 1.4 ms. The kinetics was monitored at 302 nm, the characteristic absorbance maximum of peroxynitrite ($\varepsilon_{302\ nm} = 1.705 \times 10^3\ M^{-1}\ cm^{-1}$) [50, 51, 55, 56]. Kinetic data were obtained in the absence and presence of HSA-heme-Fe(III) (final concentration 5.0×10^{-6}–4.0×10^{-5} M), CO_2 (final concentration 1.2×10^{-3} M) isoniazid (final concentration 2.0×10^{-4}–1.0×10^{-2} M), and rifampicin (final concentration 4.0×10^{-5}–5.0×10^{-4} M) by rapid mixing of the HSA-heme-Fe(III) buffered solution with the peroxynitrite solution (final concentration 2.5×10^{-4} M). The kinetics was obtained at pH 7.2 (1.0×10^{-1} M phosphate buffer) and 20.0 °C; no gaseous phase was present.

The kinetics of peroxynitrite isomerization by HSA-heme-Fe(III) in the absence and presence of CO_2, isoniazid, and rifampicin was analyzed in the framework of the minimum reaction mechanism (Scheme 1) [33, 53, 59].

Values of the pseudo-first-order rate constant for HSA-heme-Fe(III)-mediated peroxynitrite isomerization (i.e., l_{obs}) were determined in the absence and presence of CO_2, isoniazid, and rifampicin, at pH 7.2 and 20.0 °C, from the analysis of the time-dependent absorbance decrease at 302 nm, according to Eq. 5 [33, 53, 59]:

$$[\text{peroxynitrite}]_t = [\text{peroxynitrite}]_i \times e^{-l_{obs} \times t} \quad (5)$$

Values of the second-order rate constant for HSA-heme-Fe(III)-mediated peroxynitrite isomerization (i.e., l_{on}) and of the first-order rate constant for peroxynitrite isomerization in the absence of HSA-heme-Fe(III) (i.e., l_0) were determined in the absence and presence of CO_2, isoniazid, and rifampicin, at pH 7.2 and 20.0 °C, from the linear dependence of l_{obs} on the HSA-heme-Fe(III) concentration according to Eq. 6 [33, 53, 59, 60]:

$$l_{obs} = l_{on} \times [\text{HSA-heme-Fe(III)}] + l_0 \quad (6)$$

Values of l_0 for peroxynitrite isomerization in the absence of HSA-heme-Fe(III) were also determined in the

Scheme 1 Minimum reaction mechanism for peroxynitrite isomerization by HSA-heme-Fe(III)

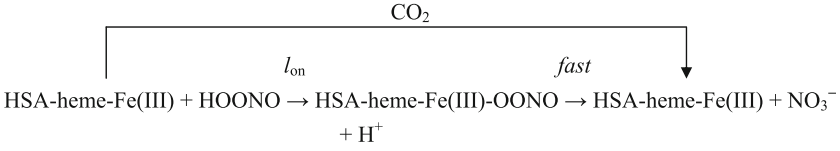

absence and presence of CO_2, isoniazid, and rifampicin, at pH 7.2 and 20.0 °C, from the analysis of the time-dependent absorbance decrease at 302 nm, according to Eq. 7 [33, 53, 59]:

$$[\text{peroxynitrite}]_t = [\text{peroxynitrite}]_i \times e^{-l_0 \times t} \quad (7)$$

Values of K_h were determined, at pH 7.2 and 20.0 °C, from the dependence of l_{on} on the drug concentration (i.e., isoniazid concentration ranging between 2.0×10^{-4} and 1.0×10^{-2} M, and rifampicin concentration ranging between 4.0×10^{-5} and 5.0×10^{-4} M). The effect of the drug concentration on l_{on} was analyzed according to Eq. 8 [33, 53, 59, 60]:

$$l_{on} = l_{on(top)} - \left(\left(l_{on(top)} \times [\text{drug}]\right)/(K_h + [\text{drug}])\right) \quad (8)$$

where $l_{on(top)}$ represents the value of l_{on} under conditions where [drug] = 0 (i.e., $l_{on(top)} = l_{on}$).

Determination of NO_2^- and NO_3^- concentration

NO_2^- and NO_3^- analysis was carried out spectrophotometrically at 543 nm by using the Griess reagent and VCl_3 to catalyze the conversion of NO_3^- to NO_2^-, as described previously [33, 59, 61, 62]. Calibration curves were obtained by measuring four to eight standard sodium nitrite and sodium nitrate solutions in 1.0×10^{-1} M phosphate buffer, pH 7.2 and 20.0 °C. The samples were prepared by mixing 500 µL of a HSA-heme-Fe(III) solution (initial concentration 1.0×10^{-4} M in 2.0×10^{-1} M phosphate buffer, pH 7.2) with 500 µL of a peroxynitrite solution (initial concentration 4.0×10^{-4} M in 0.01 M NaOH) with vortexing, at 20.0 °C, in the absence and presence of CO_2 (1.2×10^{-3} M), isoniazid (1.0×10^{-2} M), and rifampicin (5.0×10^{-4} M). The reaction mixture was analyzed within approximately 10 min.

Peroxynitrite-mediated formation of nitro-L-tyrosine in the absence and presence of HSA-heme-Fe(III), CO_2, isoniazid, and rifampicin

The reaction of peroxynitrite with free L-tyrosine was carried out at pH 7.2, at both 20.0 and 37.0 °C, by adding 0.2 mL of an alkaline (1.0×10^{-2} M NaOH) solution of peroxynitrite (2.0×10^{-3} M) to 1.8 mL of a buffered (1.0×10^{-1} M phosphate buffer) solution of L-tyrosine (final concentration 1.0×10^{-4} M) in the absence and presence of HSA-heme-Fe(III) (final concentration 5.0×10^{-6}–5.0×10^{-5} M), CO_2 (final concentration 1.2×10^{-3} M), isoniazid (final concentration 2.0×10^{-4}–1.0×10^{-2} M), and rifampicin (final concentration 4.0×10^{-5}–5.0×10^{-4} M). The amount of nitro-L-tyrosine was determined by high-performance liquid chromatography, as previously reported [33].

Values of K_h were determined from the dependence on the drug concentration of the relative yield of nitro-L-tyrosine formed from the reaction of peroxynitrite with free L-tyrosine in the absence and presence of HSA-heme-Fe(III), i.e., Y = [yield with added HSA-heme-Fe(III)/yield with no HSA-heme-Fe(III)] × 100 [33]. The effect of the isoniazid and rifampicin concentration on Y was analyzed according to Eq. 9 [33]:

$$Y = (((100 - R) \times [\text{drug}])/(K_h + [\text{drug}])) + R \quad (9)$$

where R corresponds to Y in the absence of the drug.

Data analysis

Kinetic and thermodynamic data were analyzed using the MATLAB program (The MathWorks, Natick, MA, USA). The results are given as mean values of at least four experiments plus or minus the corresponding standard deviation.

Docking analysis

Simulated automatic flexible ligand docking to HSA was performed by using Autodock 4.0 and the graphical user interface AutoDockTools [63–65]. The structure of HSA–warfarin was downloaded from the Protein Data Bank (code 2BXD) [7]. The isoniazid structure bound to cytosolic soybean ascorbate peroxidase was downloaded from the Protein Data Bank (code 2VCF) [66]. The rifampicin geometry in complex with *Thermus aquaticus* core RNA polymerase was downloaded from the Protein Data Bank (code 1I6V) [67]. Single bonds were allowed to rotate freely during the Monte Carlo simulated annealing procedure. The analysis of the conformational space was restricted to a cubic box of 60 Å edge centered on the coordinates of warfarin. Monte Carlo simulated annealing was performed by starting from a temperature of 900 K with a relative cooling factor of 0.95 per cycle to reach the temperature of 5 K in 100 cycles [63–65].

Results

Isoniazid and rifampicin binding to HSA

Isoniazid and rifampicin binding to HSA was investigated by analyzing the perturbation of the intrinsic tryptophan fluorescence of HSA that arises from the unique tryptophan residue located near Sudlow's site I in subdomain IIA, at position 214 (Fig. 1). Isoniazid induces a perturbation of the intrinsic tryptophan fluorescence of HSA similar to that induced by rifampicin [58] (data not shown), as already reported for the binding of several drugs, including warfarin, to Sudlow's site I [2, 6, 8, 9, 21, 22, 57, 68, 69].

Therefore, the perturbation of the tryptophan fluorescence of HSA appears to be essentially drug-independent [2, 6, 8, 9, 21, 22, 57, 68].

Figure 2 shows the binding isotherms for isoniazid and rifampicin association to HSA at pH 7.2 and 20.0 °C. The analysis of the data given in Fig. 2, according to Eq. 1, allowed the determination of K_0 values for isoniazid and rifampicin binding to HSA [$(3.9 \pm 0.4) \times 10^{-4}$ and $(1.3 \pm 0.1) \times 10^{-5}$ M, respectively]. The Hill coefficient (n) for isoniazid and rifampicin binding to HSA is 1.00 ± 0.02, indicating that drug binding to HSA is a noncooperative event.

Isoniazid and rifampicin binding to HSA-heme-Fe(III)

Isoniazid and rifampicin binding to HSA-heme-Fe(III) was investigated by analyzing the perturbation of the electronic absorption spectra of HSA-heme-Fe(III). Note that Sudlow's site I and the heme cleft (Fig. 1) are spectroscopically and structurally linked [8, 9, 21, 22, 34]. Isoniazid and rifampicin induce a very similar decrease in the absorption coefficient and a superimposable blueshift of the maximum of the electronic absorption spectrum of HSA-heme-Fe(III) (data not shown), as already reported for drug binding to Sudlow's site I (e.g., warfarin). Therefore, the perturbation of the electronic absorption spectra of HSA-heme-Fe(III) appears to be essentially drug-independent [8, 9, 21, 22, 34, 69].

Figure 2 shows the binding isotherms for isoniazid and rifampicin association to HSA-heme-Fe(III) at pH 7.2 and 20.0 °C. The analysis of the data given in Fig. 2, according to Eq. 2, allowed the determination of K_h values for isoniazid and rifampicin binding to HSA-heme-Fe(III) [$(4.3 \pm 0.4) \times 10^{-3}$ and $(1.2 \pm 0.1) \times 10^{-4}$ M, respectively].

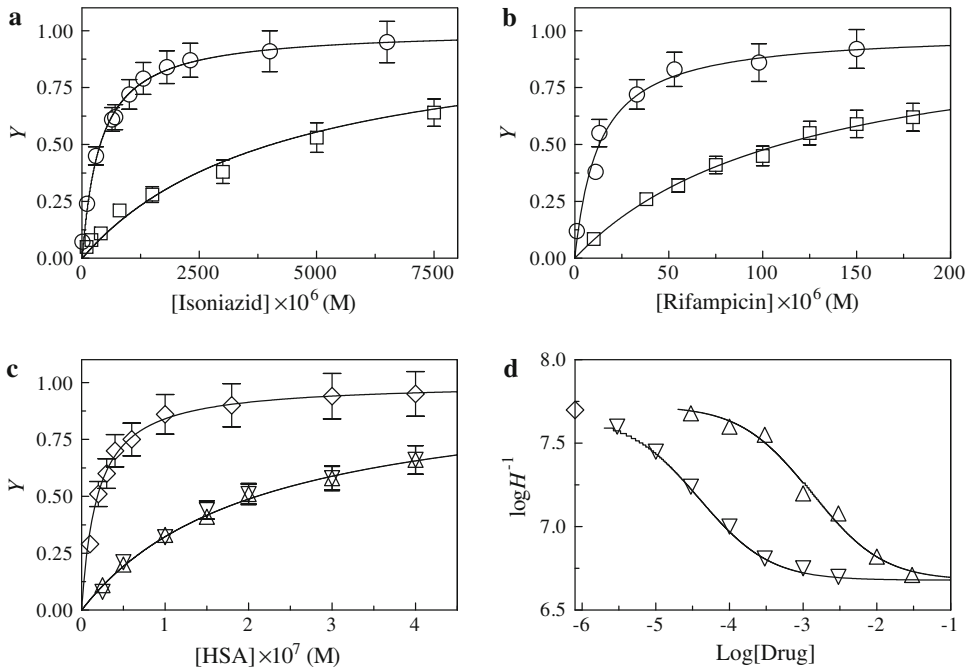

Fig. 2 Isoniazid and rifampicin binding to HSA and ferric human serum heme–albumin [HSA-heme-Fe(III)]. **a** Thermodynamics of isoniazid binding to HSA (*circles*) and HSA-heme-Fe(III) (*squares*). The *lines* were calculated according to Eqs. 1 and 2 by nonlinear regression curve fitting with $K_0 = (3.9 \pm 0.4) \times 10^{-4}$ M and $K_h = (4.3 \pm 0.4) \times 10^{-3}$ M. The isoniazid concentration corresponds to that of the free ligand. The HSA and HSA-heme-Fe(III) concentrations were 5.0×10^{-6} M. **b** Thermodynamics of rifampicin binding to HSA (*circles*) and HSA-heme-Fe(III) (*squares*). The *lines* were calculated according to Eqs. 1 and 2 by nonlinear regression curve fitting with $K_0 = (1.3 \pm 0.1) \times 10^{-5}$ M and $K_h = (1.2 \pm 0.1) \times 10^{-4}$ M. The rifampicin concentration corresponds to that of the free ligand. The HSA and HSA-heme-Fe(III) concentrations were 5.0×10^{-6} M. **c** Thermodynamics of ferric heme [heme-Fe(III)] binding to HSA in the absence (*diamonds*) and presence of isoniazid (*upward triangles*) and rifampicin (*downward triangles*). The *lines* were calculated according to Eq. 3 by nonlinear regression curve fitting with $H_0 = (1.9 \pm 0.2) \times 10^{-8}$ M and $H_d = (2.1 \pm 0.2) \times 10^{-7}$ M. The HSA concentration corresponds to that of the free ligand; the heme-Fe(III) concentration was 5.0×10^{-7} M, the isoniazid concentration was 3.0×10^{-2} M, and the rifampicin concentration was 3.0×10^{-3} M. **d** Dependence of the apparent association equilibrium constant H for heme-Fe(III) binding to HSA on the isoniazid (*upward triangles*) and rifampicin (*downward triangles*) concentrations. The *diamond* indicates the H_0^{-1} value for HSA binding to heme-Fe(III) in the absence of drugs. The *lines* were calculated according to Eq. 4 by nonlinear regression curve fitting with the following sets of parameters: isoniazid—$H_d^{-1} = (4.8 \pm 0.5) \times 10^6$ M^{-1}, $K_0 = (3.9 \pm 0.4) \times 10^{-4}$ M, and $K_h = (4.3 \pm 0.4) \times 10^{-3}$ M; and rifampicin—$H_d^{-1} = (4.8 \pm 0.5) \times 10^6$ M^{-1}, $K_0 = (1.3 \pm 0.1) \times 10^{-5}$ M, and $K_h = (1.2 \pm 0.1) \times 10^{-4}$ M. The isoniazid and rifampicin concentrations correspond to the concentration of the free ligand. Where not shown, the standard deviation is smaller than the symbol. Data were obtained at pH 7.2 and 20.0 °C. For further details, see the text

The Hill coefficient (n) for isoniazid and rifampicin binding to HSA-heme-Fe(III) is 1.00 ± 0.03, indicating that drug binding to HSA-heme-Fe(III) is a noncooperative event.

As already reported for the association of several drugs to Sudlow's site I, heme-Fe(III) inhibits isoniazid and rifampicin binding to HSA, K_0 being lower than K_h by about 1 order of magnitude (Fig. 2). Notably, this phenomenon is essentially drug-independent [8, 9, 21, 22, 26, 34, 38, 69].

Heme-Fe(III) binding to HSA and HSA–drug complexes

Heme-Fe(III) binding to HSA in the absence and presence of isoniazid and rifampicin was investigated by analyzing the perturbation of the electronic absorption spectrum of heme-Fe(III). The absorption coefficient and the maximum of the electronic absorption spectra of HSA-heme-Fe(III)–isoniazid and HSA-heme-Fe(III)–rifampicin complexes are lower and blueshifted with respect to those of the drug-free HSA-heme-Fe(III). Furthermore, the electronic absorption spectra of HSA-heme-Fe(III)–drug complexes appear to be drug-independent [8, 9, 21, 22, 34].

Figure 2 shows the binding isotherms for heme-Fe(III) association to HSA in the absence and presence of isoniazid and rifampicin at pH 7.2 and 20.0 °C. The analysis of data given in Fig. 2, according to Eq. 3, allowed the determination of H_0 and H_d values for heme-Fe(III) binding to HSA in the absence and presence of the drugs, respectively. The value of H_0 for heme-Fe(III) binding to HSA ($1.9 \pm 0.2 \times 10^{-8}$ M) agrees with the values reported in the literature [2, 8, 21, 22, 34]. Isoniazid and rifampicin inhibit heme-Fe(III) binding to HSA, H_0 being lower than H_d by about 1 order of magnitude (Fig. 2). The values of H_d for heme-Fe(III) binding to HSA in the presence of saturating levels of isoniazid and rifampicin [$H_d = (2.1 \pm 0.2) \times 10^{-7}$ M; present study], as well as of several drugs all binding to Sudlow's site I (e.g., warfarin), appear to be essentially drug-independent [8, 9, 21, 22, 26, 34, 38, 69]. Both in the absence and in the presence of isoniazid and rifampicin, the Hill coefficient (n) for heme-Fe(III) binding to HSA is 1.00 ± 0.03, indicating that drug binding to HSA-heme-Fe(III) is a noncooperative event.

According to linked functions [45], the values of H_d, K_0, and K_h obtained experimentally (Fig. 2) are in excellent agreement with those calculated according to Eq. 4 (Fig. 2), thus giving confidence that the assumptions underlying Eq. 4 are correct.

Effect of isoniazid and rifampicin on HSA-heme-Fe(III)-mediated peroxynitrite isomerization

The kinetics of peroxynitrite isomerization in the absence and presence of HSA-heme-Fe(III), CO_2, isoniazid, and rifampicin was recorded by single-wavelength stopped-flow apparatus. Under all the experimental conditions, a decrease of the absorbance at 302 nm was observed, as previously reported [33]. The kinetics of peroxynitrite isomerization was fitted to a single-exponential decay for more than 95% of its course (see Eq. 5). According to the literature [33], this indicates that no intermediate species [e.g., HSA-heme-Fe(III)-OONO; see Scheme 1] accumulate(s) in the course of peroxynitrite isomerization. In particular, the formation of the transient HSA-heme-Fe(III)–OONO species represents the rate-limiting step in catalysis, the conversion of the HSA-heme-Fe(III)–OONO complex to HSA-heme-Fe(III) and NO_3^- being faster by at least 1 order of magnitude.

In the absence and presence of CO_2, isoniazid, and rifampicin, the observed rate constants for HSA-heme-Fe(III)-catalyzed isomerization of peroxynitrite (i.e., l_{obs}) increase linearly with the HSA-heme-Fe(III) concentration (Fig. S2). The analysis of the data reported in Fig. 3, according to Eq. 6, allowed the determination of the values of the second-order rate constant for peroxynitrite isomerization by HSA-heme-Fe(III) (i.e., l_{on}, corresponding to the slope of the linear plots) and of the first-order rate constant for peroxynitrite isomerization in the absence of HSA-heme-Fe(III) (i.e., l_0, corresponding to the y intercept of the linear plots). The values of l_0 obtained according to Eq. 6 are in excellent agreement with those experimentally determined according to Eq. 7 (see Table 1). In the absence of the drugs, the values of l_{on} and l_0 for peroxynitrite isomerization in the absence and presence of CO_2 are in excellent agreement with those reported in the literature [33].

The values of l_{on} for HSA-heme-Fe(III)-catalyzed isomerization of peroxynitrite are essentially unaffected by CO_2 (Fig. 3, Table 1). In contrast, the value of l_0 for peroxynitrite isomerization obtained in the presence of CO_2 ($15.9\ s^{-1}$) is higher by about 2 orders of magnitude than that obtained in the absence of CO_2 ($2.8 \times 10^{-1}\ s^{-1}$) (Table 1). The lack of a CO_2-linked effect on peroxynitrite isomerization by HSA-heme-Fe(III) is likely related to the fact that peroxynitrite reacts faster with HSA-heme-Fe(III) ($l_{on} = 4.1 \times 10^5$ and $I_{on} = 4.3 \times 10^5\ M^{-1}\ s^{-1}$ in the absence and presence of CO_2, respectively; Table 1) than with CO_2 ($l_{on} = 3 \times 10^4\ M^{-1}\ s^{-1}$) [55, 56, 70, 71].

In the absence and presence of CO_2, isoniazid and rifampicin affect dose-dependently the l_{on} values for HSA-heme-Fe(III)-mediated isomerization of peroxynitrite (Fig. 3). Indeed, the values of l_{on} for HSA-heme-Fe(III)-catalyzed isomerization of peroxynitrite decrease from $4.1 \times 10^5\ M^{-1}\ s^{-1}$ in the absence of drugs and CO_2 to $1.3 \times 10^5\ M^{-1}\ s^{-1}$ at an isoniazid concentration of 1.0×10^{-2} M, and to $1.1 \times 10^5\ M^{-1}\ s^{-1}$ at a rifampicin concentration of 5.0×10^{-4} M. Moreover, the values of

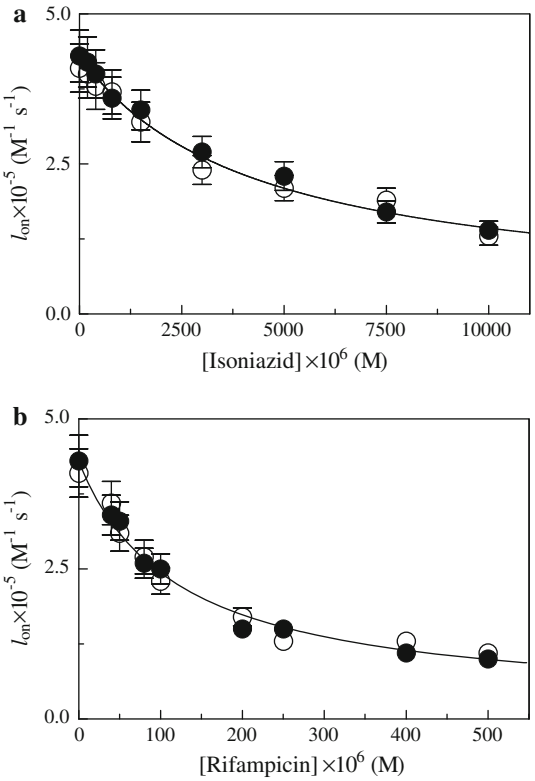

Fig. 3 Inhibition of HSA-heme-Fe(III)-mediated peroxynitrite isomerization by isoniazid (**a**) and rifampicin (**b**). Effect of the isoniazid and the rifampicin concentration on the second-order rate constant for HSA-heme-Fe(III)-catalyzed isomerization of peroxynitrite (i.e., l_{on}) in the absence (*open circles*) and presence (*filled circles*) of CO_2. The *lines* were calculated according to Eq. 8 with the following parameters: isoniazid—$l_{on(top)} = (4.2 \pm 0.3) \times 10^5$ M^{-1} s^{-1} and $K_h = (4.3 \pm 0.4) \times 10^{-3}$ M; rifampicin—$l_{on(top)} = (4.2 \pm 0.3) \times 10^5$ M^{-1} s^{-1} and $K_h = (1.2 \pm 0.1) \times 10^{-4}$ M. Where not shown, the standard deviation is smaller than the symbol. Data were obtained at pH 7.2 and 20.0 °C. For details, see the text

l_{on} decrease from 4.3×10^5 M^{-1} s^{-1} in the absence of drugs and in the presence of CO_2 to 1.4×10^5 M^{-1} s^{-1} at an isoniazid concentration of 1.0×10^{-2} M, and to 1.0×10^5 M^{-1} s^{-1} at a rifampicin concentration of 5.0×10^{-4} M (Fig. 3, Table 1). By contrast, the values of l_0 are unaffected by isoniazid and rifampicin, being only dependent on CO_2 (Fig. 3, Table 1).

According to Eq. 8 (Fig. 3), the analysis of the dependence of l_{on} for HSA-heme-Fe(III)-catalyzed isomerization of peroxynitrite on the isoniazid and rifampicin concentrations allowed the determination of the CO_2-independent values of K_h for isoniazid and rifampicin binding to HSA-heme-Fe(III) [$(4.3 \pm 0.4) \times 10^{-3}$ and $(1.2 \pm 0.1) \times 10^{-4}$ M, respectively]. The Hill coefficient (n) for isoniazid and rifampicin binding to HSA-heme-Fe(III) is 1.00 ± 0.02, indicating that drug binding to HSA-heme-Fe(III) is a noncooperative event.

Under conditions where the drug concentration is much greater than K_h, HSA-heme-Fe(III) does not catalyze the isomerization of peroxynitrite as observed in the presence of noncatalytic HSA and HSA-heme-Fe(III)–cyanide [33].

Analysis of the nitrogen-containing products of HSA-heme-Fe(III)-mediated peroxynitrite isomerization

According to the literature [33, 53, 59], the spontaneous isomerization of peroxynitrite yields $74 \pm 5\%$ NO_3^- and $24 \pm 4\%$ NO_2^-. In the presence of HSA-heme-Fe(III), the NO_3^- and NO_2^- yields increase (approximately 90%) and decrease (approximately 10%), respectively. The same result has been observed in the presence of HSA-heme-Fe(III) and CO_2. Lastly, isoniazid and rifampicin do not significantly affect the NO_3^- and NO_2^- yields (Table 2).

Isoniazid and rifampicin inhibit HSA-heme-Fe(III)-based protection of free L-tyrosine against peroxynitrite-mediated nitration

HSA-heme-Fe(III) protects dose-dependently free L-tyrosine against peroxynitrite-mediated nitration [33]. As shown in Fig. 4, isoniazid and rifampicin inhibit in a dose-dependent fashion the HSA-heme-Fe(III)-based protection of free L-tyrosine against peroxynitrite-mediated nitration in the absence and presence of CO_2. In fact, the relative yield of nitro-L-tyrosine increases on increasing the isoniazid and rifampicin concentrations at fixed HSA-heme-Fe(III), peroxynitrite, L-tyrosine, and CO_2 concentrations.

According to Eq. 9 (Figs. 4, S3), the analysis of the dependence on the isoniazid and rifampicin concentrations of the relative yield of nitro-L-tyrosine formed from the reaction of peroxynitrite with free L-tyrosine (Y) allowed the determination of the CO_2-independent values of K_h for isoniazid and rifampicin binding to HSA-heme-Fe(III) [$(3.6 \pm 0.4) \times 10^{-3}$ and $(1.7 \pm 0.2) \times 10^{-4}$ M, respectively, at 20.0 °C; and $(4.3 \pm 0.4) \times 10^{-3}$ and $(2.1 \pm 0.2) \times 10^{-4}$ M, respectively, at 37.0 °C]. Under all the experimental conditions, the Hill coefficient (n) for isoniazid and rifampicin binding to HSA-heme-Fe(III) ranges between 0.98 ± 0.02 and 1.01 ± 0.02, indicating that drug binding to HSA-heme-Fe(III) is a noncooperative event. Note that the data obtained at 20.0 °C agree with those determined at 37.0 °C (see Figs. 4, S3). Under conditions where the drug concentration is much greater than K_h, HSA-heme-Fe(III) does not protect free L-tyrosine against peroxynitrite-mediated nitration.

As expected, the values of K_h obtained spectrophotometrically (Fig. 2) and from the dependence of l_{on} on the isoniazid and rifampicin concentrations (Fig. 3) are in excellent agreement with those obtained from the dependence of the relative yield of nitro-L-tyrosine formed from the reaction of peroxynitrite with free L-tyrosine on the drug concentration (Figs. 4, S3).

Table 1 Effect of the isoniazid and rifampicin concentrations on l_0 and l_{on} values for ferric human serum heme–albumin [HSA-heme-Fe(III)]-mediated peroxynitrite isomerization in the absence and presence of CO_2 at pH 7.2 and 20.0 °C

Isoniazid (M)	l_0 or l_0^d (s^{-1})[a]		l_{on} or l_{on}^d (M^{-1} s^{-1})		Rifampicin (M)	l_0 or l_0^d (s^{-1})[a]		l_{on} or l_{on}^d (M^{-1} s^{-1})	
	$-CO_2$	$+CO_2$[b]	$-CO_2$	$+CO_2$[b]		$-CO_2$	$+CO_2$[b]	$-CO_2$	$+CO_2$[b]
0.0[c]	0.28[c]	15.9[c]	4.1×10^5[c]	4.3×10^5[c]	0.0[c]	0.28[c]	15.9[c]	4.1×10^5[c]	4.3×10^5[c]
	0.26	*16.3*				*0.26*	*16.3*		
2.0×10^{-4}	0.29	17.2	4.0×10^5	4.2×10^5	4.0×10^{-5}	0.29	17.2	3.6×10^5	3.4×10^5
	0.31	*15.9*				*0.28*	*18.9*		
4.0×10^{-4}	0.27	16.9	3.8×10^5	4.0×10^5	5.0×10^{-5}	0.27	16.9	3.1×10^5	3.3×10^5
	0.25	*18.4*				*0.24*	*17.5*		
8.0×10^{-4}	0.31	15.2	3.7×10^5	3.6×10^5	8.0×10^{-5}	0.31	15.2	2.7×10^5	2.6×10^5
	0.28	*16.9*				*0.23*	*15.8*		
1.5×10^{-3}	0.26	18.4	3.2×10^5	3.4×10^5	1.0×10^{-4}	0.26	18.4	2.3×10^5	2.5×10^5
	0.27	*16.3*				*0.27*	*19.1*		
3.0×10^{-3}	0.25	20.3	2.4×10^5	2.7×10^5	2.0×10^{-4}	0.25	20.3	1.7×10^5	1.5×10^5
	0.28	18.4				*0.26*	*19.8*		
5.0×10^{-3}	0.30	17.6	2.1×10^5	2.3×10^5	2.5×10^{-4}	0.30	17.6	1.3×10^5	1.5×10^5
	0.27	*16.5*				*0.28*	*16.9*		
7.5×10^{-3}	0.28	18.1	1.9×10^5	1.7×10^5	4.0×10^{-4}	0.28	18.1	1.3×10^5	1.1×10^5
	0.26	*19.3*				*0.29*	*17.4*		
1.0×10^{-2}	0.26	16.5	1.3×10^5	1.4×10^5	5.0×10^{-4}	0.26	16.5	1.1×10^5	1.0×10^5
	0.27	*18.8*				*0.25*	*16.6*		

[a] In regular style are shown values of l_0 and l_0^d for HSA-heme-Fe(III)-catalyzed peroxynitrite isomerization. In *italics* are shown values of l_0 and l_0^d for peroxynitrite isomerization obtained in the absence of HSA-heme-Fe(III)

[b] The CO_2 concentration was 1.2×10^{-3} M

[c] Under conditions where the drug concentration is 0.0 M, $l_0 = l_0^d$, and $l_{on} = l_{on}^d$

Table 2 NO_3^- and NO_2^- distribution of peroxynitrite isomerization in the absence and presence of HSA-heme-Fe(III), CO_2, isoniazid, and rifampicin at pH 7.2 and 20.0 °C

HSA-heme-Fe(III) (M)	CO_2 (M)	Isoniazid (M)	Rifampicin (M)	NO_3^- (%)	NO_2^- (%)	$NO_3^- + NO_2^-$ (%)
–	–	–	–	74 ± 5	24 ± 4	98
–	1.2×10^{-3}	–	–	86 ± 5	15 ± 3	101
–	–	1.0×10^{-2}	–	77 ± 5	23 ± 3	100
–	1.2×10^{-3}	1.0×10^{-2}		85 ± 3	15 ± 3	100
–	–	–	5.0×10^{-4}	73 ± 5	28 ± 3	101
–	1.2×10^{-3}	–	5.0×10^{-4}	84 ± 8	15 ± 3	99
5.0×10^{-5}	–	–	–	88 ± 5	13 ± 3	101
5.0×10^{-5}	1.2×10^{-3}	–	–	92 ± 4	7 ± 3	99
5.0×10^{-5}	–	1.0×10^{-2}		91 ± 5	9 ± 3	100
5.0×10^{-5}	1.2×10^{-3}	1.0×10^{-2}		89 ± 4	12 ± 3	101
5.0×10^{-5}	–	–	5.0×10^{-4}	92 ± 3	7 ± 4	99
5.0×10^{-5}	1.2×10^{-3}	–	5.0×10^{-4}	90 ± 4	12 ± 3	102

Automated docking simulation of isoniazid and rifampicin binding to HSA

An automated docking analysis of isoniazid and rifampicin was performed in Sudlow's site I (FA7) of HSA to confirm that these drugs could easily bind to this site (Fig. 5). Isoniazid, a small ligand, binds to the FA7 subchamber, where the coumarinic ring of warfarin is located, with an interaction energy of -24.3 kJ mol^{-1}, in agreement with that calculated from K_0. On the other hand, rifampicin only partially enters into Sudlow's site I opening that recognizes the benzyl group of warfarin. Therefore, this prevents the

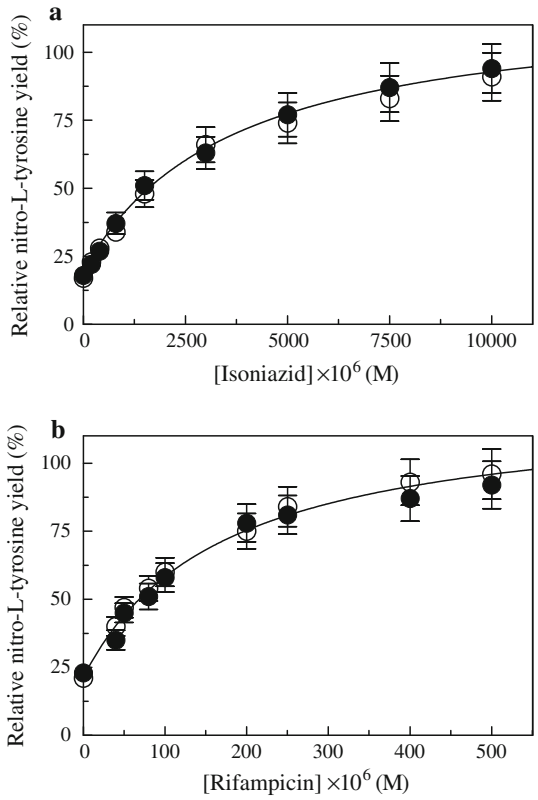

Fig. 4 Effect of isoniazid (**a**) and rifampicin (**b**) concentrations on the relative yield of nitro-L-tyrosine formed from the reaction of peroxynitrite with free L-tyrosine at pH 7.2 and 20.0 °C in the presence of HSA-heme-Fe(III) and in the absence (*open circles*) and presence (*filled circles*) of CO_2. The *lines* were calculated according to Eq. 9 with the following parameters: **a** $K_h = (3.6 \pm 0.4) \times 10^{-3}$ M and $R = 19.3 \pm 1.7\%$; and **b** $K_h = (1.7 \pm 0.2) \times 10^{-4}$ M and $R = 21.3 \pm 2.0\%$. The concentrations of HSA-heme-Fe(III), peroxynitrite, free L-tyrosine, and CO_2 were 2.5×10^{-5}, 2.0×10^{-3}, 1.0×10^{-4}, and 1.2×10^{-3} M, respectively. Where not shown, the standard deviation is smaller than the symbol. For details, see the text

determination of the rifampicin docking energy. It should be noticed, however, that the simulation does not take into account induced-fit conformational changes involving the protein backbone [64].

Discussion

Isoniazid and rifampicin bind noncooperatively to Sudlow's site I, as suggested by the drug-dependent quenching of the intrinsic HSA fluorescence [6, 21, 22, 57, 58, 69]. As expected for Sudlow's site I ligands, both antituberculosis drugs modulate allosterically heme-Fe(III) binding to HSA as well as peroxynitrite isomerization by HSA-heme-Fe(III), highlighting the role of heterotropic ligands in modulating the HSA(-heme) reactivity [8, 32, 48, 72].

The affinity of isoniazid and rifampicin for HSA decreases by about 1 order of magnitude in the presence of saturating amounts of heme-Fe(III) (Fig. 2). Further, as expected on the basis of linked functions [45], the heme-Fe(III) affinity for HSA decreases by about 1 order of magnitude in the presence of saturating amounts of isoniazid and rifampicin (Fig. 2). Accordingly, the difference in the reaction free energy for drug binding to HSA in the absence and presence of heme-Fe(III) [$\delta\Delta G^\circ = -RT \ln(K_0/K_h) = 5.6 \pm 0.2$ kJ mol^{-1}] is similar to the difference in the reaction free energy for heme-Fe(III) binding to HSA in the absence and presence of drugs [$\delta\Delta G^\circ = -RT \ln(H_0/H_d) = 5.8$ kJ mol^{-1}] at pH 7.2 and 20.0 °C. This value, which is essentially drug-independent [8, 9, 21, 22, 26, 34, 38, 69], indicates that the interaction energy between the Sudlow's site I and FA1, where the heme binds, is 5.7 kJ mol^{-1} independent of the affinity of the drug for Sudlow's site I; this value likely reflects the free energy associated with the conformational change(s) required for the structural communication between the two sites.

Peroxynitrite isomerization is facilitated by HSA-heme-Fe(III) (see the present study and [33]). However, unlike ibuprofen inhibition of HSA-heme-Fe(III) action by binding to Sudlow's site II [33], isoniazid and rifampicin impair allosterically HSA-heme-Fe(III)-mediated peroxynitrite isomerization by binding to Sudlow's site I (Fig. 5). This behavior could reflect drug-dependent structural changes occurring at the heme binding pocket of HSA. Indeed, abacavir binding to Sudlow's site I modulates peroxynitrite-mediated oxidation of ferrous nitrosylated HSA-heme [HSA-heme-Fe(II)-NO] [48]. Moreover, abacavir binding and warfarin binding to Sudlow's site I facilitate HSA-heme-Fe(II)-NO denitrosylation [31]. Both events reflect the drug-dependent neutral-to-basic conformational transition in HSA-heme-Fe(II)-NO [31, 48]. Sudlow's site I ligands interact with Tyr150 and Arg252 residues, two key residues positioned in the center of the drug binding site. In turn, Tyr150 drives the reorientation of Phe149, which is no longer available for the stabilization of the heme-Fe(III) porphyrin ring by π–π stacking, with a consequent effect on the heme-Fe(III)-based catalysis (see the present study and [9, 31, 33, 48]).

Peroxynitrite isomerization by heme-Fe(III) proteins [e.g., HSA-heme-Fe(III)] could represent a physiological detoxification mechanism, protecting cells from reactive nitrogen and oxygen species [70, 71]; this potential role is reinforced by the evidence that enzymatically active HSA-heme-Fe(III) indeed protects L-tyrosine from the nitrosylation (see Figs. 4, S3). Note that the rate of peroxynitrite isomerization by HSA-heme-Fe(III) is faster by about 1 order of magnitude than the rates reported for ferric horse heart myoglobin, sperm whale myoglobin, and human hemoglobin [33, 53, 59]. Moreover, peroxynitrite isomerization by HSA-heme-Fe(III) is faster than peroxynitrite

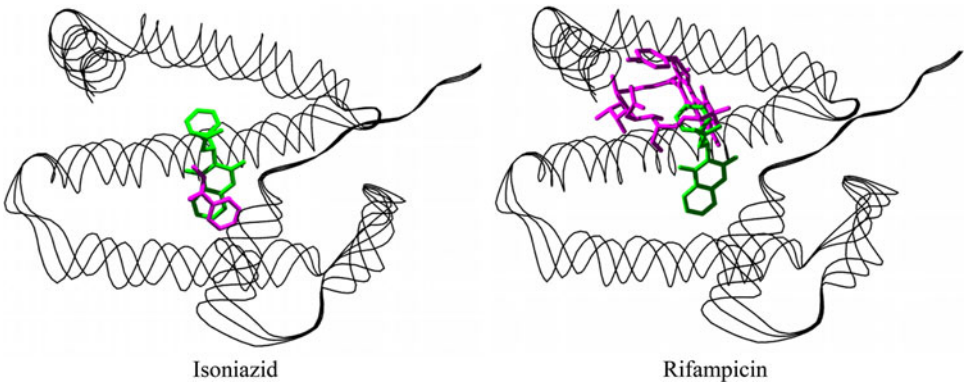

Fig. 5 Binding mode of isoniazid and rifampicin to the FA7 site of HSA. Isoniazid and rifampicin are rendered in *magenta sticks*. Warfarin, the prototypical ligand of the FA7 site (i.e., Sudlow's site I), is rendered in *green sticks*. Structural models have been obtained by simulation of automated docking of drugs into the FA7 binding cleft of the HSA structure (Protein Data Bank code 2BXD [7]). For details, see the text

scavenging by ferrous nitrosylated heme proteins, which appears to be strongly limited by (1) the dissociation of the heme-Fe(III)–NO transient and (2) the reduction of the final heme-Fe(III) species to the ferrous heme derivative [33, 48].

Owing to the role of HSA in human plasma [1–9], some in vivo implications could be argued from the present results:

1. Peroxynitrite isomerization by HSA-heme-Fe(III) could occur only in patients affected by diseases where a relevant intravascular hemolysis takes place. Under these pathological conditions, the HSA-heme-Fe(III) plasma level increases from the physiological concentration (approximately 1×10^{-6} M) to approximately 4×10^{-5} M [20, 73]. To mimic as much as possible this condition, the HSA-heme-Fe(III) concentration here used ranged from 5.0×10^{-6} to 5.0×10^{-5} M.
2. Although the in vivo concentration of peroxynitrite is openly debated, the level of peroxynitrite in the reperfused ischemic heart has been reported to be much higher than micromolar concentration, at least over a brief period of time [70, 71], overlapping the lowest peroxynitrite concentration here used (2.5×10^{-5} M).
3. Accounting for the plasma HSA concentration (approximately 7.5×10^{-4} M) [2], the plasma levels of isoniazid and rifampicin (ranging between 1×10^{-5} and 1×10^{-4} M [74, 75]), and the values of K_0 and K_h determined here, the molar fraction of the drug-bound HSA and HSA-heme-Fe(III) could range between 10 and 50%.

Any inhibitory effect on peroxynitrite isomerization by HSA-heme-Fe(III) results in a relevant effect on the putative HSA detoxification role. The fact that several drugs binding at different sites of HSA might reduce this potentially important role should induce some caution for the simultaneous drug administration employed for several therapeutic protocols. Thus, this control should be carried out routinely to avoid some paradoxical therapeutic effect, as for the management of antituberculosis therapy. Indeed, the increase of the plasma levels of heme-Fe(III) under pathological conditions [20, 72] may induce a release of antituberculosis drugs; accordingly, the toxic free-heme plasma concentration could increase in patients under antituberculosis drug therapy. Moreover, the protective role of HSA-heme-Fe(III), catalyzing peroxynitrite detoxification, could be impaired by antituberculosis drugs; this could facilitate the peroxynitrite-mediated nitration of aromatic residues (such as Tyr), which represents a relevant posttranslational protein modification process [70, 71, 76].

Acknowledgments This work was partially supported by grants from the Ministero dell'Istruzione, dell'Università e della Ricerca of Italy (PRIN 2007ECX29E_002 and University Roma Tre, CLAR 2009, to P.A.) and from the Ministero della Salute of Italy (Istituto Nazionale per le Malattie Infettive I.R.C.C.S. 'Lazzaro Spallanzani', Ricerca corrente 2009 to P.A.).

References

1. Sudlow G, Birkett DJ, Wade DN (1975) Mol Pharmacol 11:824–832
2. Peters T Jr (ed) (1996) All about albumin: biochemistry, genetics and medical applications. Academic Press, San Diego
3. Curry S (2002) Vox Sang 83(Suppl 1):315–319
4. Kragh-Hansen U, Chuang VT, Otagiri M (2002) Biol Pharm Bull 25:695–704
5. Sakurai Y, Ma SF, Watanabe H, Yamaotsu N, Hirono S, Kurono Y, Kragh-Hansen U, Otagiri M (2004) Pharm Res 21:285–292
6. Sułkowska A, Bojko B, Równicka J, Sułkowski W (2004) Biopolymers 74:256–262
7. Ghuman J, Zunszain PA, Petitpas I, Bhattacharya AA, Otagiri M, Curry S (2005) J Mol Biol 353:38–52

8. Ascenzi P, Bocedi A, Notari S, Fanali G, Fesce R, Fasano M (2006) Mini Rev Med Chem 6:483–489
9. Ascenzi P, Fasano M (2010) Biophys Chem 148:16–22
10. Curry S, Mandelkov H, Brick P, Franks N (1998) Nat Struct Biol 5:827–835
11. Sugio S, Kashima A, Mochizuki S, Noda M, Kobayashi K (1999) Protein Eng 12:439–446
12. Yamasaki K, Maruyama T, Yoshimoto K, Tsutsumi Y, Narazaki R, Fukuhara A, Kragh-Hansen U, Otagiri M (1999) Biochim Biophys Acta 1432:313–323
13. Bhattacharya AA, Curry S, Franks NP (2000) J Biol Chem 275:38731–38738
14. Bhattacharya AA, Grüne T, Curry S (2000) J Mol Biol 303:721–732
15. Petitpas I, Bhattacharya AA, Twine S, East M, Curry S (2001) J Biol Chem 276:22804–22809
16. Chuang VTG, Otagiri M (2002) Pharm Res 19:1458–1464
17. Hamilton JA (2004) Prog Lipid Res 43:177–199
18. Lejon S, Frick IM, Björck L, Wikström M, Svensson S (2004) J Biol Chem 279:42924–42928
19. Curry S (2009) Drug Metab Pharmacokinet 24:342–357
20. Miller YI, Shaklai N (1999) Biochim Biophys Acta 1454:153–164
21. Ascenzi P, Bocedi A, Notari S, Menegatti E, Fasano M (2005) Biochem Biophys Res Commun 334:481–486
22. Bocedi A, Notari S, Menegatti E, Fanali G, Fasano M, Ascenzi P (2005) FEBS J 272:6287–6296
23. Fasano M, Fanali G, Leboffe L, Ascenzi P (2007) IUBMB Life 59:436–440
24. Fasano M, Baroni S, Vannini A, Ascenzi P, Aime S (2001) J Biol Inorg Chem 6:650–658
25. Wardell M, Wang Z, Ho JX, Robert J, Rüker F, Ruble J, Carter DC (2002) Biochem Biophys Res Commun 291:813–819
26. Nicoletti FP, Howes BD, Fittipaldi M, Fanali G, Fasano M, Ascenzi P, Smulevich G (2008) J Am Chem Soc 130:11677–11688
27. Komatsu T, Matsukawa Y, Tsuchida E (2000) Bioconjug Chem 11:772–776
28. Monzani E, Bonafé B, Fallarini A, Redaelli C, Casella L, Minchiotti L, Galliano M (2001) Biochim Biophys Acta 1547:302–312
29. Kamal JK, Behere DV (2002) J Biol Inorg Chem 7:273–283
30. Komatsu T, Ohmichi N, Nakagawa A, Zunszain PA, Curry S, Tsuchida E (2005) J Am Chem Soc 127:15933–15942
31. Ascenzi P, Imperi F, Coletta M, Fasano M (2008) Biochem Biophys Res Commun 369:686–691
32. Fasano M, Fanali G, Fesce R, Ascenzi P (2008) In: Bolognesi M, di Prisco G, Verde C (eds) Dioxygen binding and sensing proteins. Springer, Heidelberg, pp 121–131
33. Ascenzi P, di Masi A, Coletta M, Ciaccio C, Fanali G, Nicoletti FP, Smulevich G, Fasano M (2009) J Biol Chem 284:31006–31017
34. Baroni S, Mattu M, Vannini A, Cipollone R, Aime S, Ascenzi P, Fasano M (2001) Eur J Biochem 268:6214–6220
35. Mattu M, Vannini A, Coletta M, Fasano M, Ascenzi P (2001) J Inorg Biochem 84:293–296
36. Fasano M, Mattu M, Coletta M, Ascenzi P (2002) J Inorg Biochem 91:487–490
37. Monzani E, Curto M, Galliano M, Minchiotti L, Aime S, Baroni S, Fasano M, Amoresano A, Salzano AM, Pucci P, Casella L (2002) Biophys J 83:2248–2258
38. Fanali G, Fesce R, Agrati C, Ascenzi P, Fasano M (2005) FEBS J 272:4672–4683
39. Fanali G, Bocedi A, Ascenzi P, Fasano M (2007) FEBS J 274:4491–4502
40. Fanali G, De Sanctis G, Gioia M, Coletta M, Ascenzi P, Fasano M (2009) J Biol Inorg Chem 14:209–217
41. Fanali G, Pariani G, Ascenzi P, Fasano M (2009) FEBS J 276:2241–2250
42. Kragh-Hansen U, Watanabe H, Nakajou K, Iwao Y, Otagiri M (2006) J Mol Biol 363:702–712
43. Simard JR, Zunszain PA, Hamilton JA, Curry S (2006) J Mol Biol 361:336–351
44. du Toit LC, Pillay V, Danckwerts MP (2006) Respir Res 7:118
45. Wyman J Jr (1964) Adv Protein Chem 19:223–286
46. Kharitonov VG, Sharma VS, Magde D, Koesling D (1997) Biochemistry 36:6814–6818
47. Boffi A, Das TK, Della Longa S, Spagnolo C, Rousseau DL (1999) Biophys J 77:1143–1149
48. Ascenzi P, Fasano M (2007) Biochem Biophys Res Commun 353:469–474
49. Notari S, Mancone C, Sergi M, Gullotta F, Bevilacqua N, Tempestilli M, Urso R, Lauria FN, Pucillo LP, Tripodi M, Ascenzi P (2010) IUBMB Life 62:387–393
50. Bohle DS, Glassbrenner PA, Hansert B (1996) Methods Enzymol 269:302–311
51. Koppenol WH, Kissner R, Beckman JS (1996) Methods Enzymol 269:296–302
52. Herold S, Exner M, Boccini F (2003) Chem Res Toxicol 16:390–402
53. Herold S, Kalinga S, Matsui T, Watanabe Y (2004) J Am Chem Soc 126:6945–6955
54. Ascenzi P, Visca P (2008) Methods Enzymol 436:317–337
55. Goldstein S, Merényi G (2008) Methods Enzymol 436:49–61
56. Goldstein S, Lind J, Merényi G (2005) Chem Rev 105:2457–2470
57. Bocedi A, Notari S, Narciso P, Bolli A, Fasano M, Ascenzi P (2004) IUBMB Life 56:609–614
58. Yang JD, Deng SX, Liu ZF, Kong L, Liu SP (2007) Luminescence 22:559–566
59. Herold S, Kalinga S (2003) Biochemistry 42:14036–14046
60. Herold S, Matsui T, Watanabe Y (2001) J Am Chem Soc 123:4085–4086
61. Miranda KM, Espey MG, Wink DA (2001) Nitric Oxide 5:62–71
62. Ascenzi P, Bocedi A, Bolognesi M, Fabozzi G, Milani M, Visca P (2006) Biochem Biophys Res Commun 339:450–456
63. Goodsell DS, Olson AJ (1990) Proteins 8:195–202
64. Goodsell DS, Morris GM, Olson AJ (1998) J Mol Recogn 9:1–5
65. Morris GM, Goodsell DS, Halliday RS, Huey R, Hart WE, Belew RK, Olson AJ (1998) J Comput Chem 19:1639–1662
66. Metcalfe C, Macdonald IK, Murphy EJ, Brown KA, Raven EL, Moody PC (2008) J Biol Chem 283:6193–6200
67. Campbell EA, Korzheva N, Mustaev A, Murakami K, Nair S, Goldfarb A, Darst SA (2001) Cell 104:901–912
68. Maes V, Engelborghs Y, Hoebeke J, Maras Y, Vercruysse A (1982) Mol Pharmacol 21:100–107
69. Fanali G, Rampoldi V, di Masi A, Bolli A, Lopiano L, Ascenzi P, Fasano M (2010) IUBMB Life 62:371–376
70. Herold S, Fago A (2005) Comp Biochem Physiol A Mol Integr Physiol 142:124–129
71. Ascenzi P, di Masi A, Sciorati C, Clementi E (2010) Biofactors 36:264–273
72. Fasano M, Curry S, Terreno E, Galliano M, Fanali G, Narciso P, Notari S, Ascenzi P (2005) IUBMB Life 57:787–796
73. Muller-Eberhard U, Javid J, Liem HH, Hanstein A, Hanna M (1968) Blood 32:811–815
74. Houin G, Beucler A, Richelet S, Brioude R, Lafaix C, Tillement JP (1983) Ther Drug Monit 5:67–72
75. Delahunty T, Lee B, Conte JE (1998) J Chromatogr B Biomed Sci Appl 705:323–329
76. Alvarez B, Radi R (2003) Amino Acids 25:295–311
77. Pfeiffer S, Gorren AC, Schmidt K, Werner ER, Hansert B, Bohle DS, Mayer B (1997) J Biol Chem 272:3465–3470
78. Zunszain PA, Ghuman J, Komatsu T, Tsuchida E, Curry S (2003) BMC Struct Biol 3:6